atoms

MDPI

Article

Electron and Positron Impact Ionization of $SF_{6-n}H_n(n = 0 - 6)$; $\{SCl_n, SF_{n-1}Cl(n = 1 - 6)\}$ and SF_5X $(X = CN, CFO)$

S. Suriyaprasanth [1], Heechol Choi [2] and Dhanoj Gupta [1,*]

[1] Department of Physics, School of Advanced Sciences, Vellore Institute of Technology University, Vellore 632014, Tamil Nadu, India; suriyaprasanth.s@vit.ac.in
[2] Institute of Plasma Technology, Korea Institute of Fusion Energy, 37 Dongjangsan-ro, Gunsan 54004, Jeollabuk-do, Republic of Korea; hcchoi@kfe.re.kr
* Correspondence: dhanoj.gupta@vit.ac.in

Abstract: We have calculated the electron and positron impact ionization of a set of molecules, $SF_{6-n}H_n(n = 0 - 6)$, $SCl_n(n = 1 - 6)$, $SF_{n-1}Cl(n = 1 - 6)$ and SF_5X $(X = CN, CFO)$, for which there are much fewer data in the literature. We have optimized the targets, and their electric polarizability is calculated along with their orbital binding and kinetic energies within the Hartree–Fock approximation that serve as input to the Binary Encounter Bethe (BEB) model for both electron and positron ionization. Most of the targets are investigated for the first time, apart from SF_6, for which we compared our data with various experimental and theoretical data, giving us a good comparison.

Keywords: electron impact; positron impact; BEB model; ionization; SF_6 alternatives

Citation: Suriyaprasanth, S.; Choi, H.; Gupta, D. Electron and Positron Impact Ionization of $SF_{6-n}H_n(n = 0 - 6)$; $\{SCl_n, SF_{n-1}Cl(n = 1 - 6)\}$ and SF_5X $(X = CN, CFO)$. *Atoms* **2023**, *11*, 137. https://doi.org/10.3390/atoms11100137

Academic Editor: Jean-Christophe Pain

Received: 13 September 2023
Revised: 13 October 2023
Accepted: 19 October 2023
Published: 21 October 2023

1. Introduction

The collisions of electrons with atoms, molecules, ions, and surfaces are of fundamental importance in low-temperature plasmas (LTPs), with numerous applications in plasma science and technologies. SF_6 gas has many uses in industry, especially as an electrically insulating gas in high-voltage environments, and it is also used in gas-insulated voltage switchgears and gas-insulated lines [1,2]. SF_6 serves as a good dielectric in high-voltage industrial applications like power transmission and is used as a feedstock gas in the semiconductor industry for etching purposes. A mixture of SF_6 with tetrafluoroethane ($C_2H_2F_4$) and other gaseous refrigerants such as R134a are being used in resistive plate chambers in neutrino and dark matter detectors and also in photosensitive gaseous detectors [3]. Despite having many applications in the plasma industry, one major drawback of SF_6 is its higher global warming potential (GWP), which is 22,800 times larger than that of CO_2, and it is tough to decompose in the atmosphere [4]. It is found that for every gram of SF_6 gas released into the atmosphere, the hazard it causes is equivalent to every 22.5 kg of CO_2 gas [5]. Moreover, owing to the Kyoto protocol's [6] requirement for the reduced emission of perfluorocarbons and SF_6, research is being conducted on new gases with a lower GWP that can be suitable substitutes for existing plasma gases. Numerous scattering studies have been conducted on several perfluorocarbons (PFCs), perfluoroketons (PFKs), and perfluoronitriles (PFNs) that could be potential alternatives to or replacements for SF_6 [7–9]. A recent review article also highlighted the possible replacement gases for SF_6 [10]. Any substitute for the SF_6 must posses a low GWP, high dielectric strength, good thermal stability, and lower ozone-depleting potential (ODP) [11,12], and should also have a lower electron attachment cross-sections [13]. It should be noted here that most of the targets investigated contain fluorine as one of the constituent atoms, which could indirectly damage the ozone layer. As there are no studies of GWP and ODP for the targets investigated here, one can also look into these properties in future studies. Rejoub et al. [14] experimentally investigated the electron impact dissociative ionization of SF_x^+ $(x = 1 - 6)$ and F^+ using a time-of-flight (TOF) mass spectrometer with a position-sensitive detector (PSD)

from first ionization energy until 1000 eV, in which the partial ionization cross-sections (PICS) were summed up to give total ionization cross-sections (TICS). Bull et al. [15,16] also experimentally provided the PICS of the fragment cations of SF_6, and the sum of the PICS gives the TICS of the parent molecule, SF_6 . Antony and coworkers employed the spherical complex optical potential (SCOP) and complex scattering potential-ionization contribution (CSP-ic) [17] methods to calculate electron impact TICS for SF_6 [18] and several other similar molecules, including SF_n $(n = 1 - 5)$ [19,20]. They also presented a review article on positron scattering on atoms and molecules [21]. The National Institute of Standards and Technology (NIST) web book contains electron impact BEB TICS for molecules such as SF_n $(n = 1 - 6)$ and many more atoms and molecules [22]. The Deutsch-Märk (DM) model [23,24] is another method that is used to calculate the electron impact TICS for atomic and molecular targets. Jain and Khare [25,26] also provided a model to study electron scattering on atoms, molecules, and clusters. Zhang et al. proposed a new method of combining the BEB model and the DM model to predict the TICS that give close agreement with the experimental results [8]. Also, Bartschat et al. showed [27] a way to calculate electron impact ionization cross-sections using the R-matrix method for atoms, which is computationally expensive. In this work, we have used the BEB model, where no fitting parameters are used to calculate electron impact TICS, which was originally formulated by Kim et al. [28]; for positron impact TICS, we used the various modified BEB models formulated by Fedus et al. [29] and Franz et al. [30]. In recent years, the BEB method has been very successful in calculating TICS for various molecules ranging from diatomic [31] to organic molecules [32], with applications in plasma and biological sciences.

Here, we present the total electron/positron impact TICS for the following set of molecular targets: $SF_{6-n}H_n$ $(n = 0 - 6)$, $(SCl_n,\ SF_{n-1}Cl) : (n = 1 - 6)$, and SF_5CN, SF_5CFO. There are no studies available for ionization for these molecular targets, and they could be viable replacements for SF_6 in plasma application. Yu et al. [33] studied the dielectric strength and boiling point of $SF_{6-n}H_n$ $(n = 0 - 6)$, SF_5CN, SF_5CFO. Leiding et al. performed quantum chemical studies on bonding and isomerism on SCl_n, $SF_{n-1}Cl$ $(n = 1 - 6)$ [34,35]. The literature survey indicates a lack of TICS for these targets, which has motivated us to take up this study to provide the TICS for both electron and positron impacts. The optimized structures of the molecular targets studied are presented in Figure 1. In the sections to follow, we describe the methodology in Section 2, present the results and discussion in Section 3, and conclude our findings in Section 4.

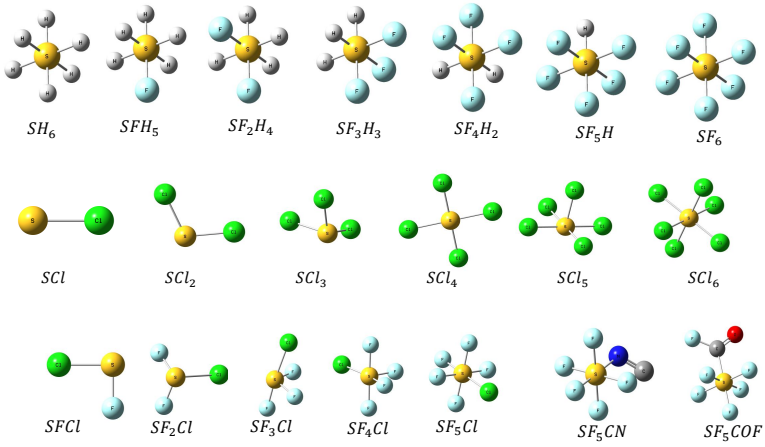

Figure 1. Structure of the molecular targets where the different colors represent different atoms: chlorine (green), sulfur (yellow), fluorine (cyan), oxygen (red), nitrogen (navy), hydrogen (light gray), and carbon (gray).

2. Binary Encounter Bethe (BEB) Model

The BEB model [28] is one of the standard approaches for determining the TICS for atoms, molecules, and ions. The BEB method calculates the electron impact TICS for each

orbital, and the sum of the cross-sections for each orbital in index (i) gives the TICS for a target under consideration.

$$\sigma(E) = \sum_{i}^{N} \sigma_i(E)\,, \tag{1}$$

The BEB method can also be used to model the direct positron impact ionization of atoms and molecules with the Binary Encounter Dipole (BED) model combined with the Wannier-type threshold law [36] to give a simple analytical formula for ionization [29,30]. The BEB model is the simplified version of the BED [28] model. The difference between the two models is the exclusion of the differential dipole oscillator strengths (DOS), which is required for each molecular orbital of the target atom or molecule in the BED model. There are also several other versions of the BEB model to calculate the single differential cross-section [37–39] and a modified version of the BEB model which also accounts for the relativistic effects [40,41]. But, here, we have employed the simplified BEB model, which does not require values of continuum DOS, $\frac{df}{dW}$. The BEB formula for the determination of the TICS is as follows:

$$\sigma_i^{BEB}(E) = \frac{S}{(t_i + u_i + 1)/n}\left[\frac{Q_i \ln t_i}{2}\left(1 - \frac{1}{t_i^2}\right) + (2 - Q_i)\left\{\left(1 - \frac{1}{t_i}\right) - \frac{\ln t_i}{t_i + 1}\right\}\right] \tag{2}$$

The reduced variables t_i, u_i, Q_i and S are as follows:

$$S = 4\pi a_0^2 N (R/B)^2, u_i = U/B, t_i = E/B$$

$$Q_i = \frac{2}{N}\int \frac{B}{B+W}\,\frac{df}{dW}\,dW$$

Here, n is the principal quantum number, W is the ejected electron's kinetic energy, and Q_i is the dipole constant defined in terms of DOS. When we lack the information on $\frac{df}{dW}$, then we can assume $Q_i = 1$ for the simplified BEB model. The incident kinetic energy is (E), the Bohr radius is $(a_0 = 0.52918\ \AA)$, and the Rydberg constant is $(R = 13.6057\ \text{eV})$. The orbital binding energy is (B), the orbital kinetic energies are (U), and the orbital occupation number is (N). To calculate the orbital parameters required as input to the BEB method, we first optimized the target molecules using the density functional theory (DFT) with the functional $\omega B97X - D$ with the aug-cc-PVTZ basis set, which calculates the energy minima at which the molecule is more stable. After optimization, the orbital binding and kinetic energies are calculated using the Hartree–Fock (HF)-type approximation. The magnitudes of BEB TICS calculated using the parameters obtained by means of DFT functionals tend to be higher than the experimental TICS [7]; hence, they are not utilized in our present study. The BEB TICS calculated using the orbital parameters obtained from the HF approximation seem reasonable and are found to give cross-section values within the uncertainty of 10–15% of the experimental values of TICS [42]. All the quantum chemistry calculations are performed using the Gaussian-16 [43] quantum chemistry package.

The BEB model for direct positron impact ionization is given by Fedus et al. [29], who modified the analytical BEB model for electrons of Kim et al. [28]. The BEB model introduced by Fedus et al. [29] for positron impact are called $BEB - 0$ and $BEB - W$ models. The equation where there is no effect of the scaling term, i.e., $C = 0$, from which it got the name $BEB - 0$, is given in Equation (3):

$$\sigma_i^{BEB-0}(E) = \frac{S_i}{t_i + u_i + 1}\left[\frac{\ln t_i}{2}\left(1 - \frac{1}{t_i^2}\right) + 1 - \frac{1}{t_i}\right], \tag{3}$$

In the $BEB-W$ model, a scaling factor (f_i^W) is incorporated that controls how the cross-section behaves at energies that are just above the ionization threshold and guarantees that the cross-section obeys the Wannier law $\sigma(E) \propto (E-B)^{1.127}$. Hence, this model is called the $BEB-W$ model, and is given below:

$$\sigma_i^{BEB-W}(E) = \frac{S_i}{t_i + u_i + 1 + f_i^W}\left[\frac{\ln t_i}{2}\left(1 - \frac{1}{t_i^2}\right) + 1 - \frac{1}{t_i}\right], \tag{4}$$

the scaling factor is defined as

$$f_i^W = \frac{C}{\nu^k},$$

where $\nu = (t_i - 1)$ and the power term k is 1.65, which obeys the Wannier exponent law proposed by Klar [36]. As the value of C is an unknown parameter, for simplicity, the constant C is fixed to be equal to unity, which also aligns well with the experimental data.

The BEB model for positron impact was further extended by Franz et al. [30] with the implementation of two new variants of the BEB model. The two new models introduced by Franz et al. [30] are called the $BEB-A$ and $BEB-B$ models, which implement the Jansen's threshold law [44] and are modified versions of the $BEB-0$ model as given below:

$$\sigma_i^{BEB-A}(E) = \frac{S_i}{t_i + u_i + 1 + f_i^A}\left[\frac{\ln t_i}{2}\left(1 - \frac{1}{t_i^2}\right) + 1 - \frac{1}{t_i}\right], \tag{5}$$

where the scaling factor is defined as

$$f_i^A = \frac{C'}{\nu^{\alpha-1}\,\eta},$$

Here,

$$\eta = e^{-\beta_i\sqrt{\nu}},$$

the value of α and β are fixed by Franz et al. [30],

$$\alpha = 2.640\ ,$$

$$\beta_i = 0.489\sqrt{\frac{B_i}{2R}},$$

and the value of C' is fixed to be equal to unity. The factor β_i depends on the orbital binding energy. This is due to the use of the reduced kinetic energy (t_i) in the BEB model rather than the excess kinetic energy $(\Delta E = E - B_i)$ as in the threshold law formulation.

The $BEB-B$ model of Franz et al. [30] is given below:

$$\sigma_i^{BEB-B}(E) = \frac{S_i}{t_i + u_i + 1}\left[\frac{\ln t_i}{2}\left(1 - \frac{1}{t_i^2}\right) + h_i(t_i)\left(1 - \frac{1}{t_i}\right) + g_i(t_i)\left(1 - \frac{1}{t_i}\right)^{\alpha}\right], \tag{6}$$

where the terms $g_i(t_i)$ and $h_i(t_i)$ are defined as

$$g_i(t_i) = C_i\eta,$$

$$h_i(t_i) = 1 - g_i(t_i),$$

It has been verified that the product of $g_i(t_i)$ and $h_i(t_i)$ gives Jansen's threshold law [44]. At high incident energies, a more dominant behavior of the second term is seen, which brings the cross-section to the maximum. Franz et al. [30] have found that for polar molecules, the $BEB-(0/W)$ model is reliable, and for non-polar molecules, both $BEB-(A/B)$ are in good agreement with the experimental data. Hence, the scope for the development of a more generalized model for positron impact ionization, which can

predict the cross-section for any molecule irrespective of their polar or non-polar nature, could be looked at in the near future.

3. Results

In this section, we present the numerical values of the maximum TICS for electron and positron impact in the tabular form along with the calculated polarizability and highest occupied molecular orbital (HOMO) energy for all the targets. Our calculated values are compared with the literature data and are shown in Table 1. The present HOMO energy computed in the HF approximation is compared with the ionization potential (IP) of the target available in the literature. Our values are generally higher than those of the literature data, as the HF calculations are found to predict energies that are generally higher compared to the actual IP because the effect of electron correlations are not taken into account. The polarizability calculated in the HF approximation with the aug-cc-PVTZ basis set is also provided in Table 1. Our polarizability for $SF_{6-n}H_n$ $(n = 0-6)$ compares fairly well with the data of Yu et al. [33]. For other sets SCl_n, $SF_{n-1}Cl$ $(n = 1-6)$ and SF_5CN, SF_5CFO, we could not find any comparison of the polarizability in the literature. Here, we also present the graphical representation of the TICS for the various sets of molecules investigated in this study for both electron and positron ionization. In Figure 2, we have shown the comparison of our electron impact TICS data of SF_6 with those of Bull et al. [16] and Rejoub et al. [14]; reference BEB data from the NIST Web book [22], Joshipura et al. [18], and Zhong et al. [8]; and the recommended data of Christophorou et al. [45]. Our results for electron impact ionization show good comparison with the NIST data [22] and Rejoub et al. [14] and Christophorou et al. [45] and lie close to the experimental values with 5% and 8% uncertainty in the TICS data of Bull et al. [16] and Rejoub et al. [14]. We have also shown the positron TICS computed using various models in the same plot, as we were not able to find any comparison for the same. Since SF_6 has a zero dipole moment, it is a non-polar molecule, and we recommend using the BEB-B model to predict the TICS, as it is found to match very well with the experimental results [29,30]. The good comparison of our electron impact ionization of SF_6 has inspired us to study the set of targets $SF_{6-n}H_n$ $(n = 0-6)$, SCl_n, $SF_{n-1}Cl$ $(n = 1-6)$ and SF_5CN, SF_5CFO, for which we could not find a complete set of data in the literature for both electron and positron impacts.

In Figure 3, we compare the TICS of all the molecules in the set of $SF_{6-n}H_n$ $(n = 0-6)$ for electron and positron ionization. As we can see from the plots, with the increase in the number of electrons in the target, the TICS are also increasing. However, for SH_6, we can see that its cross-section is larger than SH_5F and SH_4F_2, owing to its lower HOMO energy, as can be seen in Table 1. Since the BEB method is very sensitive to the binding energies of the valence shell orbitals, its effect is quite prominent, where the lower binding energies lead to a higher magnitude of TICS. In Figure 3b, we have shown the positron TICS for all the targets. For SX_6 $(X = H, F)$ molecules with zero dipole moment, the cross-section is calculated using the BEB-B model, and for the other molecular targets which had a nonzero dipole moment, we used the BEB-W model to calculate their positron impact TICS. There are no previous studies for these targets, and hence all the results are plotted together to obtain an idea about the shape and magnitude of the cross sections.

We have calculated the electron and positron TICS for SCl_n $(n = 1-6)$, and they are shown in Figure 4. For both electron and positron impacts, as the size of the target increases, the cross-section also increases. In this case also for non-polar molecules, such as SCl_n $(n = 4, 6)$, the cross-sections calculated using the BEB-B model are shown, and for polar molecules such as SCl_n $(n = 1, 2, 3, 5)$, the cross-sections calculated using BEB-W are plotted. Further investigation is required, as there are no data available in the literature for these targets.

Table 1. The table contains the absolute values of electric dipole polarizability, ionization energy, and the maximum cross-section; we have compared the values calculated by us with the values in the literature.

Molecule	Polarzability ($Å$)		HOMO (eV)	IP (eV)	$TICS_{max}$ (10^{-16} cm^2)	
	Present	Literature	Present	Literature	Electron	Positron
SF_6	4.033	4.490 [a], 4.04 [b]	18.450	15.33 [c], 15.320 [a], 16.5 [d], 15.6 [e]	7.415	8.304
SF_5H	4.048	4.03 [b]	16.405	–	7.021	8.264
SF_4H_2	4.107	4.07 [b]	15.619	–	6.629	7.787
SF_3H_3	4.232	4.11 [b]	13.474	–	6.310	7.417
SF_2H_4	4.446	4.28 [b]	12.704	–	6.037	7.102
SFH_5	4.902	4.61 [b]	10.198	–	6.014	7.103
SH_6	5.576	5.11 [b]	9.577	–	6.642	7.078
SCl	4.967	–	10.507	9.57 [a]	4.522	5.309
SCl_2	7.326	–	10.252	9.47 [a]	6.912	8.103
SCl_3	11.396	–	10.089	–	8.762	10.275
SCl_4	15.692	–	9.822	–	11.553	12.777
SCl_5	16.622	–	10.949	–	12.989	15.230
SCl_6	17.363	–	12.217	–	15.475	17.143
$SFCl$	5.235	–	13.900	–	5.5833	6.534
SF_2Cl	7.272	–	10.521	–	6.309	7.380
SF_3Cl	6.355	–	10.622	–	7.216	8.444
SF_4Cl	6.576	–	12.062	–	7.746	9.081
SF_5Cl	6.004	–	12.664	12.335 [a]	8.619	10.110
SF_5CN	5.985	–	14.256	–	9.037	10.638
SF_5CFO	6.026	–	14.710	–	9.726	11.433

Reference [a] [46] Reference [b] [33] Reference [c] [22] Reference [d] [45] Reference [e] [18].

Similarly, we have calculated the TICS for another set of molecules $SF_{n-1}Cl$ $(n = 1-6)$ that shows a similar behavior to previous cases, where the cross-section increases with the size of the target (number of electrons present in the target), as shown in Figure 5. For positron impact, the BEB-W model is used, as all the targets in this set are polar, and the results are shown in Figure 5b.

Two more targets, SF_5CN and SF_5CFO, that are important for plasma applications are investigated for ionization, and the results are shown in Figure 6 for electron and positron impacts. The BEB-W model is used for the calculation of positron impact TICS for these targets, as they are polar in nature.

In Figure 7, we show the comparison of the TICS for SCl_6, SF_6, and SH_6 in one plot for both electron and positron impacts. As the size of the SCl_6 is quite big, its cross-section is higher than the other two targets. However, the HOMO energy of SH_6 is lower than SF_6 by 7 to 8 eV; hence, the cross-sections for SH_6 and SF_6 are comparable even though the size of SH_6 is much smaller than SF_6. Overall, the positron impact cross-sections for all the targets are larger than the electron impact due to the negation of exchange and interference effects [47] with the target, along with the inclusion of scaling factor in the Jansen's threshold law and Wannier exponent that is used in the positron ionization.

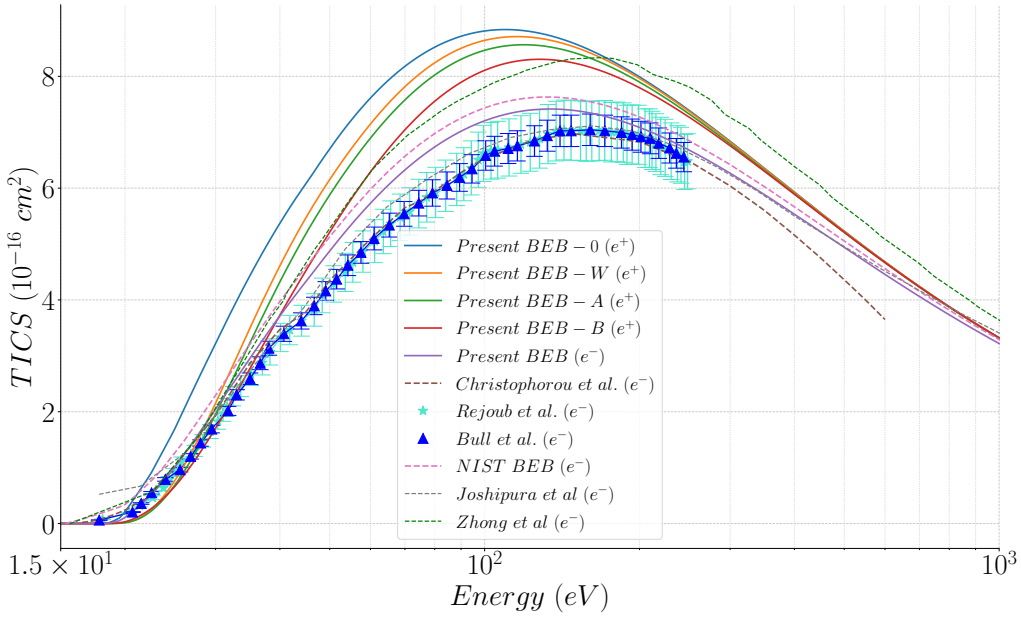

Figure 2. Electron and positron TICS of SF_6, $BEB - 0$ (blue line for positron), $BEB - W$ (orange line for positron), $BEB - A$ (green line for positron), $BEB - B$ (red line for positron), $BEB -$ (purple line for electron), Christophorou et al. (dashed brown line for electron) [45], Rejoub et al. (staZr for electron) [14], Bull et al. (upright triangle forelectron) [16], NIST BEB data (dashed pink line forelectron) [22], Joshipura et al. (dashed gray line for electron) [18], Zhong et al. (dashed green line for electron) [8].

In Figure 8, the maximum TICS for electrons and positrons are plotted with the number of electrons present for all the targets studied. For both cases, as the number of electrons increases, the maximum TICS also increase, indicated by a linear fit for all the targets.

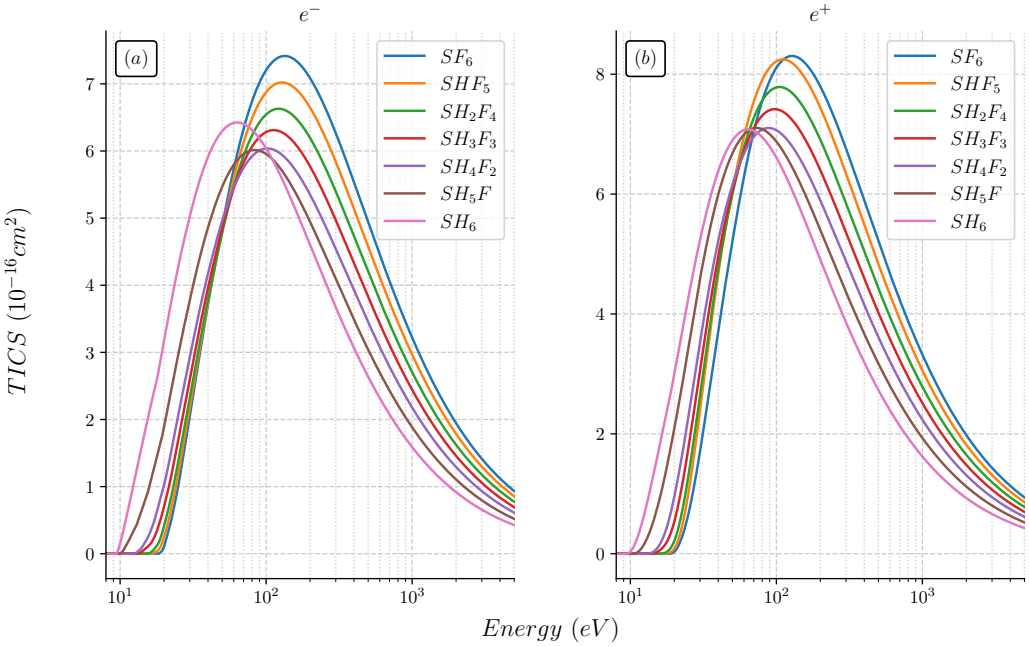

Figure 3. Total electron/positron impact ionization cross-sections of $SF_{6-x}H_x (x = 0 - 6) : SF_6\ (blue)$, $SHF_5\ (orange)$, $SH_2F_4\ (green)$, $SH_3F_3\ (red)$, $SH_4F_2\ (purple)$, $SH_5F\ (brown)$, $SH_6\ (pink)$: (**a**) the cross-section for electron impact ionization; (**b**) the cross-section for positron impact ionization.

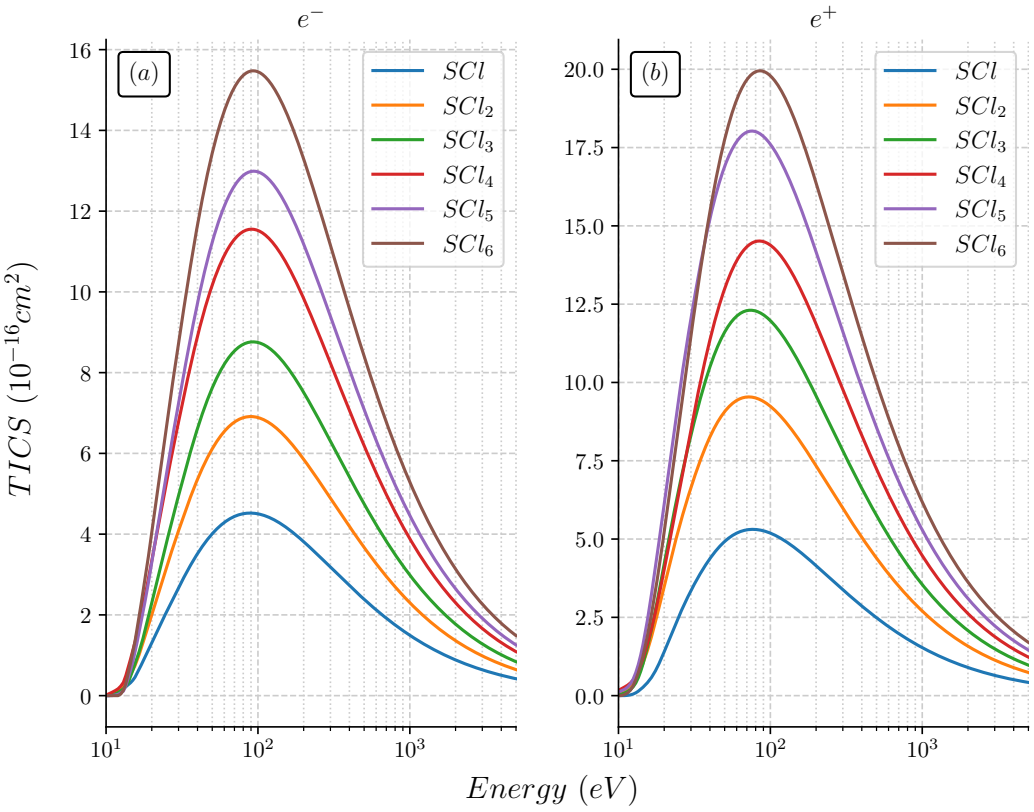

Figure 4. Total electron/positron impact ionization cross-sections of $SCl_n (n = 1 - 6)$: SCl $(blue)$, SCl_2 $(orange)$, SCl_3 $(green)$, SCl_4 (red), SCl_5 $(purple)$, SCl_6 $(brown)$: (**a**) the cross-section for electron impact ionization; (**b**) the cross-section for positron impact ionization.

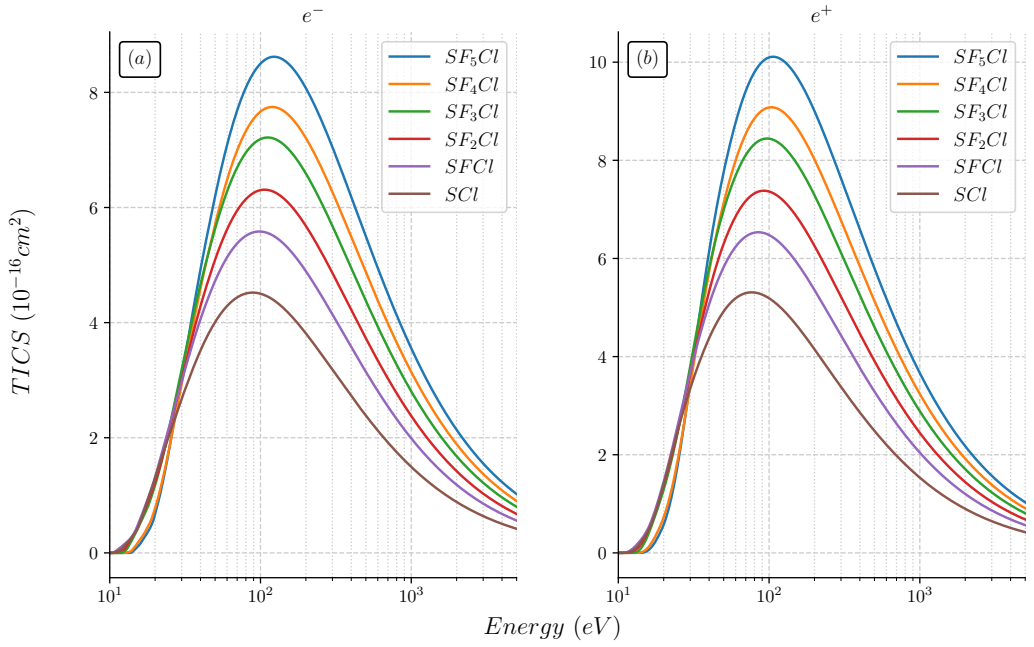

Figure 5. Total electron/positron impact ionization cross-sections of $SF_{6-n}H_n$ $(n = 1 - 6)$: $SCl(brown)$, $SFCl(purple)$, $SF_2Cl(red)$, $SF_3Cl(green)$, $SF_4Cl(orange)$, $SF_5Cl(blue)$: (**a**) the cross-section for electron impact ionization; (**b**) the cross-section for positron impact ionization.

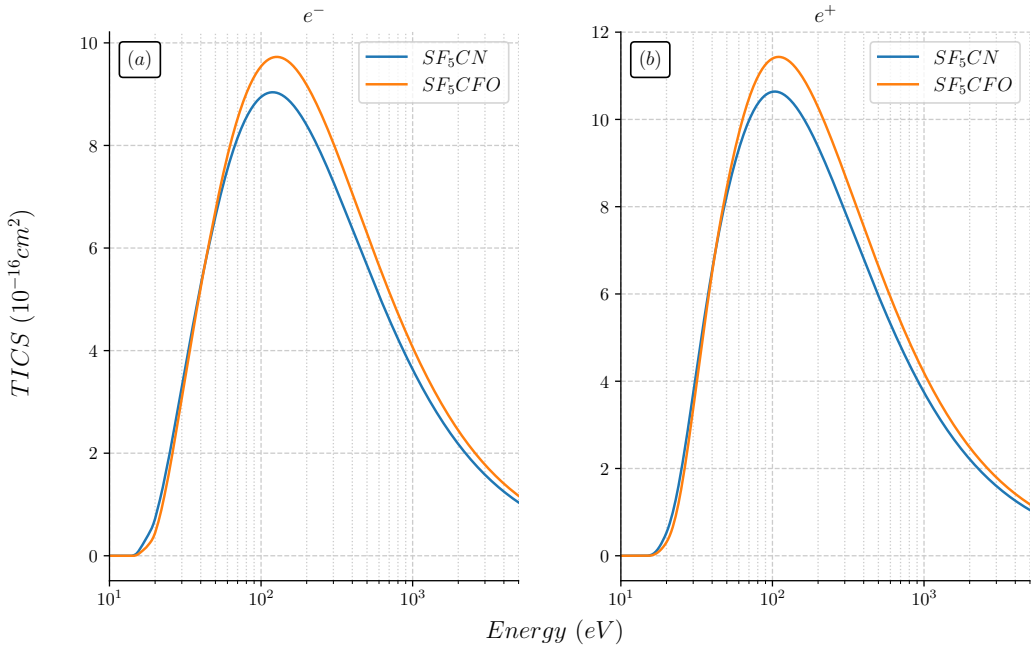

Figure 6. Total electron/positron impact ionization cross-sections of SF_5CFO (*orange*) and SF_5CN (*blue*): (**a**) the cross-section for electron impact ionization; (**b**) the cross-section for positron impact ionization.

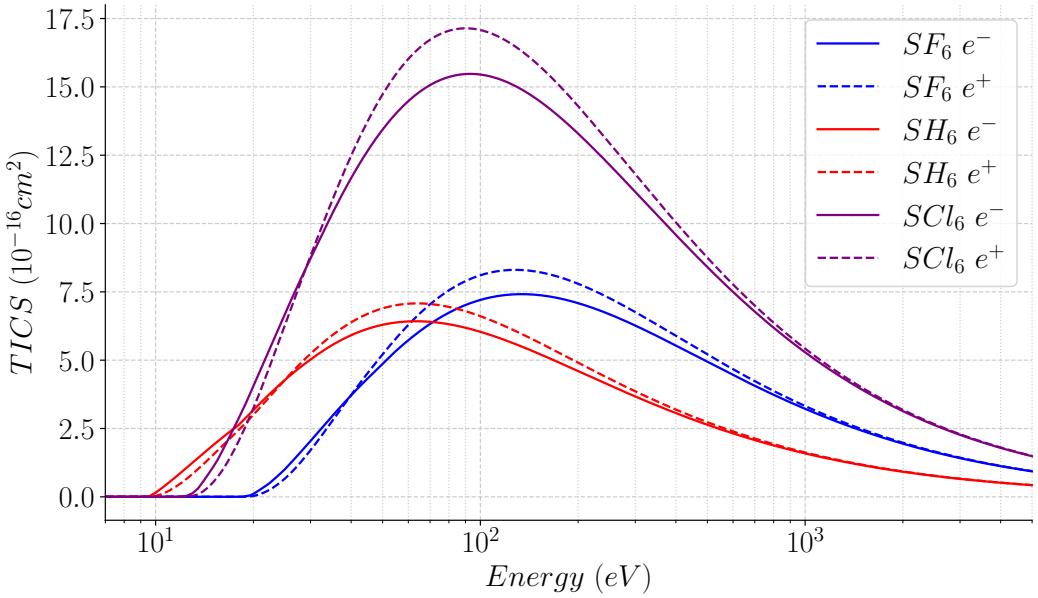

Figure 7. Comparison of the total electron and positron impact ionization cross-sections of SX_6 $X = H, Cl, F$. The solid lines represents the cross-sections calculated using the BEB model for electrons, and the dashed lines represent the cross-sections calculated using the BEB-B model for positrons.

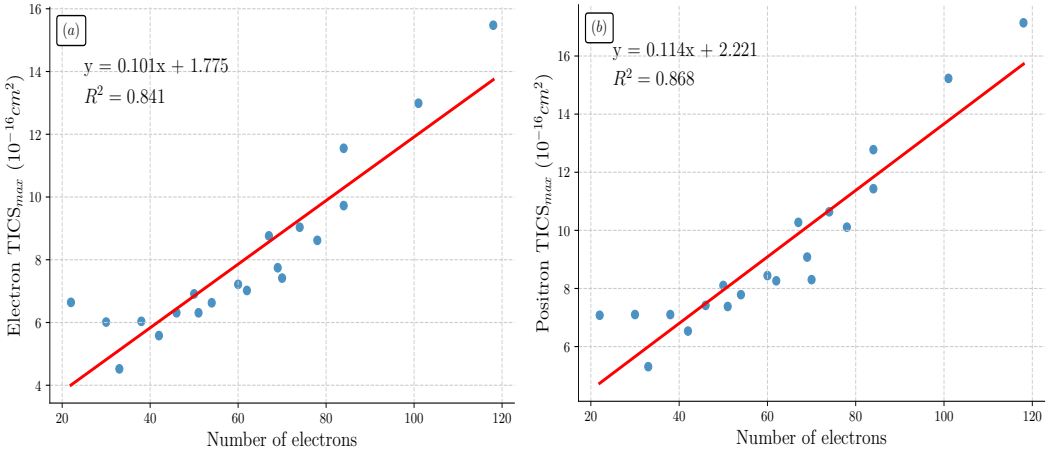

Figure 8. The figure contains the correlation plots for the size of the molecule in terms of electron number and maximum TICS. Subfigure (**a**) shows the number of electrons present vs. the maximum TICS for electron impact, and subfigure (**b**) shows the number of electrons present vs. the maximum TICS for positron impact.

4. Conclusions

We have calculated the electron and positron TICS for a set of molecules for which there are no or very few data available, and these molecules could be a viable alternative gas for SF_6 for plasma applications. The structures of the targets were optimized, and their electric dipole polarizability was calculated using HF approximations and compared with the available data, showing reasonable agreement. Our calculated electron TICS for SF_6 showed good comparison with various experimental and theoretical data, motivating us to perform calculations for targets for which there are no studies available for either electron or positron impacts. The electron impact ionization was calculated using the BEB model for electrons. For the positron TICS, we chose to use the BEB-W model for molecules with a zero dipole moment and the BEB-B model to calculate the cross-sections of molecules with a non-zero dipole moment. With respect to the theoretical predictions using the BEB method and in the absence of any experimental data for most of the targets, it is quite challenging to make an estimate of the uncertainty in the theoretical data. But our data could be trusted within 15% uncertainty, as the BEB TICS computed using the HF method are found to give good agreement with experimental results within an uncertainty of 15% [7,29,30,48–50]. We hope this study will motivate others to explore these plasma-relevant species for other collision processes along with ionization to validate our data.

Author Contributions: All the authors equally contributed in this manuscript. All authors have read and agreed to the published version of the manuscript.

Funding: This research received no external funding.

Institutional Review Board Statement: Not applicable.

Informed Consent Statement: Not applicable.

Data Availability Statement: Data will be shared upon request to the corresponding author.

Acknowledgments: S.S. acknowledges the Vellore Institute of Technology for providing a research fellowship; D.G. acknowledges the Science and Engineering Research Board (SERB), Department of Science and Technology (DST), Government of India (Grant No. SRG/2022/000394) for providing financial support and computational facilities; H.C. acknowledges support from the R&D Program of "Plasma Big Data ICT Convergence Technology Research Project (EN2342-9)" through the Republic of Korea Institute of Fusion Energy (KFE), funded by Government funds, Republic of Korea.

Conflicts of Interest: The authors declare no conflict of interest.

References

1. Nguyen, T.T.N.; Sasaki, M.; Odaka, H.; Tsutsumi, T.; Ishikawa, K.; Hori, M. Remotely floating wire-assisted generation of high-density atmospheric pressure plasma and SF_6-added plasma etching of quartz glass. *J. Appl. Phys.* **2019**, *125*, 063304 . [CrossRef]
2. Li, X.; Zhao, H.; Murphy, A.B. SF_6-alternative gases for application in gas-insulated switchgear. *J. Phys. D Appl. Phys.* **2018**, *51*, 153001. [CrossRef]
3. Matsuoka, K.; Okubo, R.; Adachi, Y. Demonstration of a 25-picosecond single-photon time resolution with gaseous photo-multiplication. *Nucl. Instrum. Methods Phys. Res. Sect. A Accel. Spectrometers Detect. Assoc. Equip.* **2023**, *1053*, 168378. [CrossRef]
4. Wang, F.; Dun, Q.; Chen, S.; Zhong, L.; Fan, X.; Li, L. Calculations of total electron impact ionization cross sections for fluoroketone and fluoronitrile. *IEEE Trans. Dielectr. Electr. Insul.* **2019**, *26*, 1693–1700. [CrossRef]
5. Tianpeng, Y.; Dong, X.; Zhou, W.; Zheng, Y.; Ren, S.; Lei, H. Study on gas molecular structure parameters based on maximum information coefficient. *IEEE Trans. Dielectr. Electr. Insul.* **2022**, *29*, 1633–1639. [CrossRef]
6. Oberthür, S.; Ott, H.E. *The Kyoto Protocol: International Climate Policy for the 21st Century*; Springer Science & Business Media: Berlin/Heidelberg, Germany, 1999.
7. Gupta, D.; Choi, H.; Song, M.Y.; Karwasz, G.P.; Yoon, J.S. Electron impact ionization cross section studies of C_2F_x ($x = 1 - 6$) and C_3F_x ($x = 1 - 8$) fluorocarbon species. *Eur. Phys. J. D* **2017**, *71*, 1–10. [CrossRef]
8. Zhong, L.; Xu, J.; Wang, X.; Rong, M. Electron-impact ionization cross sections of new SF_6 replacements: A method of combining Binary-Encounter-Bethe (BEB) and Deutsch-Märk (DM) formalism. *J. Appl. Phys.* **2019**, *126*, 193302. [CrossRef]
9. Chang, H.; Sinha, N.; Choi, H.; Song, M.Y.; Jang, H.J.; Oh, Y.H.; Song, K.D. Theoretical process for the investigation of dielectric characteristics of F3NO as an alternative gas for SF_6. *AIP Adv.* **2023**, *13*, 065215. [CrossRef]
10. Gupta, D. Brief review of electron collision studies of molecules relevant to plasma. *Appl. Sci. Converg. Technol.* **2020**, *29*, 125–132. [CrossRef]
11. Zhong, L.; Wang, J.; Wang, X.; Rong, M. Comparison of dielectric breakdown properties for different carbon-fluoride insulating gases as SF_6 alternatives. *AIP Adv.* **2018**, *8*, 085122. [CrossRef]
12. Wang, Y.; Huang, D.; Liu, J.; Zhang, Y.; Zeng, L. Alternative environmentally friendly insulating gases for SF_6. *Processes* **2019**, *7*, 216. [CrossRef]
13. Fenzlaff, M.; Gerhard, R.; Illenberger, E. Associative and dissociative electron attachment by SF_6 and SF5Cl. *J. Chem. Phys.* **1988**, *88*, 149–155. [CrossRef]
14. Rejoub, R.; Sieglaff, D.; Lindsay, B.; Stebbings, R. Absolute partial cross sections for electron-impact ionization of SF_6 from threshold to 1000 eV. *J. Phys. B At. Mol. Opt. Phys.* **2001**, *34*, 1289. [CrossRef]
15. Bull, J.N.; Lee, J.W.; Vallance, C. Absolute electron total ionization cross-sections: Molecular analogues of DNA and RNA nucleobase and sugar constituents. *Phys. Chem. Chem. Phys.* **2014**, *16*, 10743–10752. [CrossRef]
16. Bull, J.N.; Lee, J.W.; Vallance, C. Electron-impact-ionization dynamics of SF_6. *Phys. Rev. A* **2017**, *96*, 042704. [CrossRef]
17. Gupta, D.; Antony, B. Electron impact ionization of cycloalkanes, aldehydes, and ketones. *J. Chem. Phys.* **2014**, *141*, 054303. [CrossRef] [PubMed]
18. Joshipura, K.; Vinodkumar, M.; Limbachiya, C.; Antony, B. Calculated total cross sections of electron-impact ionization and excitations in tetrahedral (X Y 4) and SF 6 molecules. *Phys. Rev. A* **2004**, *69*, 022705. [CrossRef]
19. Goswami, B.; Antony, B.; Fritzsche, S. Electron impact scattering and calculated ionization cross sections for SFx (x = 1–5) radicals. *Int. J. Mass Spectrom.* **2017**, *417*, 8–15. [CrossRef]
20. Singh, S.; Gupta, D.; Antony, B. Electron and positron scattering cross sections for propene. *J. Appl. Phys.* **2018**, *124*, 034901. [CrossRef]
21. Nahar, S.N.; Antony, B. Positron scattering from atoms and molecules. *Atoms* **2020**, *8*, 29. [CrossRef]
22. Linstrom, P.J.; Mallard, W.G. The NIST Chemistry WebBook: A chemical data resource on the internet. *J. Chem. Eng. Data* **2001**, *46*, 1059–1063. [CrossRef]
23. Deutsch, H.; Märk, T.; Tarnovsky, V.; Becker, K.; Cornelissen, C.; Cespiva, L.; Bonacic-Koutecky, V. Measured and calculated absolute total cross-sections for the single ionization of CFx and NFx by electron impact. *Int. J. Mass Spectrom. Ion Process.* **1994**, *137*, 77–91. [CrossRef]
24. Deutsch, H.; Becker, K.; Matt, S.; Märk, T. Theoretical determination of absolute electron-impact ionization cross sections of molecules. *Int. J. Mass Spectrom.* **2000**, *197*, 37–69. [CrossRef]
25. Jain, D.; Khare, S. Ionizing collisions of electrons with CO_2, CO, H_2O, CH_4 and NH_3. *J. Phys. B At. Mol. Phys.* **1976**, *9*, 1429. [CrossRef]
26. Khare, S.P. *Introduction to the Theory of Collisions of Electrons with Atoms and Molecules*; Springer Science & Business Media: New York, NY, USA, 2002.
27. Bartschat, K.; Burke, P. The R-matrix method for electron impact ionisation. *J. Phys. B At. Mol. Phys.* **1987**, *20*, 3191. [CrossRef]
28. Kim, Y.K.; Rudd, M.E. Binary-encounter-dipole model for electron-impact ionization. *Phys. Rev. A* **1994**, *50*, 3954. [CrossRef]
29. Fedus, K.; Karwasz, G.P. Binary-encounter dipole model for positron-impact direct ionization. *Phys. Rev. A* **2019**, *100*, 062702. [CrossRef]

30. Franz, M.; Wiciak-Pawłowska, K.; Franz, J. Binary-Encounter Model for Direct Ionization of Molecules by Positron-Impact. *Atoms* **2021**, *9*, 99. [CrossRef]
31. Huber, S.E.; Mauracher, A.; Süß, D.; Sukuba, I.; Urban, J.; Borodin, D.; Probst, M. Total and partial electron impact ionization cross sections of fusion-relevant diatomic molecules. *J. Chem. Phys.* **2019**, *150*, 024306. [CrossRef]
32. Gupta, D.; Choi, H.; Singh, S.; Modak, P.; Antony, B.; Kwon, D.C.; Song, M.Y.; Yoon, J.S. Total ionization cross section of cyclic organic molecules. *J. Chem. Phys.* **2019**, *150*, 064313. [CrossRef]
33. Yu, X.; Hou, H.; Wang, B. Prediction on dielectric strength and boiling point of gaseous molecules for replacement of SF_6. *J. Comput. Chem.* **2017**, *38*, 721–729. [CrossRef] [PubMed]
34. Leiding, J.; Woon, D.E.; Dunning, T.H., Jr. Bonding in SCl_n ($n = 1 - 6$): A Quantum Chemical Study. *J. Phys. Chem. A* **2011**, *115*, 4757–4764. [CrossRef] [PubMed]
35. Leiding, J.; Woon, D.E.; Dunning, T.H., Jr. Bonding and Isomerism in $SF_{n-1}Cl$ ($n = 1 - 6$): A Quantum Chemical Study. *J. Phys. Chem. A* **2011**, *115*, 329–341. [CrossRef] [PubMed]
36. Klar, H. Threshold ionisation of atoms by positrons. *J. Phys. B At. Mol. Phys.* **1981**, *14*, 4165. [CrossRef]
37. Kim, Y.K.; Johnson, W.R.; Rudd, M.E. Cross sections for singly differential and total ionization of helium by electron impact. *Phys. Rev. A* **2000**, *61*, 034702. [CrossRef]
38. Guerra, M.; Amaro, P.; Machado, J.; Santos, J. Single differential electron impact ionization cross sections in the binary-encounter-Bethe approximation for the low binding energy regime. *J. Phys. B At. Mol. Opt. Phys.* **2015**, *48*, 185202. [CrossRef]
39. Garkoti, P.; Luthra, M.; Goswami, K.; Bharadvaja, A.; Baluja, K.L. The binary-encounter-Bethe model for computation of singly differential cross sections due to electron-impact ionization. *Atoms* **2022**, *10*, 60. [CrossRef]
40. Kim, Y.K.; Santos, J.P.; Parente, F. Extension of the binary-encounter-dipole model to relativistic incident electrons. *Phys. Rev. A* **2000**, *62*, 052710. [CrossRef]
41. Guerra, M.; Parente, F.; Indelicato, P.; Santos, J. Modified binary encounter Bethe model for electron-impact ionization. *Int. J. Mass Spectrom.* **2012**, *313*, 1–7. [CrossRef]
42. Karwasz, G.P.; Możejko, P.; Song, M.Y. Electron-impact ionization of fluoromethanes–Review of experiments and binary-encounter models. *Int. J. Mass Spectrom.* **2014**, *365*, 232–237. [CrossRef]
43. Frisch, M.; Trucks, G.; Schlegel, H.B.; Scuseria, G.; Robb, M.; Cheeseman, J.; Scalmani, G.; Barone, V.; Petersson, G.; Nakatsuji, H.; et al. Gaussian 16. 2016. Available online: https://gaussian.com/gaussian16/ (accessed on 12 September 2023).
44. Jansen, K.; Ward, S.; Shertzer, J.; Macek, J. Absolute cross section for positron-impact ionization of hydrogen near threshold. *Phys. Rev. A* **2009**, *79*, 022704. [CrossRef]
45. Christophorou, L.G.; Olthoff, J.K. Electron interactions with SF 6. *J. Phys. Chem. Ref. Data* **2000**, *29*, 267–330. [CrossRef]
46. Johnson, R.D., III. Computational Chemistry Comparison and Benchmark DataBase. 2022. Available online: https://cccbdb.nist.gov/ (accessed on 12 September 2023).
47. Blanco, F.; García, G. Interference effects in the electron and positron scattering from molecules at intermediate and high energies. *Chem. Phys. Lett.* **2015**, *635*, 321–327. [CrossRef]
48. Hwang, W.; Kim, Y.K.; Rudd, M.E. New model for electron-impact ionization cross sections of molecules. *J. Chem. Phys.* **1996**, *104*, 2956–2966. [CrossRef]
49. Ghosh, S.; Nixon, K.; Pires, W.; Amorim, R.; Neves, R.; Duque, H.V.; da Silva, D.; Jones, D.; Blanco, F.; Garcia, G.; et al. Electron impact ionization of 1-butanol: II. Total ionization cross sections and appearance energies. *Int. J. Mass Spectrom.* **2018**, *430*, 44–51. [CrossRef]
50. Graves, V.; Cooper, B.; Tennyson, J. Calculated electron impact ionisation fragmentation patterns. *J. Phys. B At. Mol. Opt. Phys.* **2022**, *54*, 235203. [CrossRef]